Supplement of Weather Clim. Dynam., 2, 331–357, 2021
https://doi.org/10.5194/wcd-2-331-2021-supplement

Supplement of

The role of air–sea fluxes for the water vapour isotope signals in the cold and warm sectors of extratropical cyclones over the Southern Ocean

Iris Thurnherr et al.

Correspondence to: Iris Thurnherr (iris.thurnherr@uib.no)

S1 Moisture source diagnostic

In this study, we use the moisture source diagnostic WaterSip developed by Sodemann et al. (2008), which was adjusted to identify the moisture sources of water vapour (Pfahl and Wernli, 2008) along the ACE track using seven-day $COSMO_{iso}$ backward trajectories. The same setup as in Aemisegger et al. (2014) is used, which includes the following steps:

- The changes in specific humidity q are analyses along the backward trajectories. For each 1 h time step along the trajectories, the change Δq to the previous time step is calculated. If $\Delta q > 0\,\mathrm{g\,kg^{-1}}$, i.e. an increase in q compared to the previous time step, the uptake of moisture by the air parcel is assumed to be caused by ocean evaporation. An increase in q while the air parcel was above the marine boundary layer (MBL) is also considered to be a signal from ocean evaporation as convective updrafts can introduce MBL moisture to altitudes well above the MBL top (for details see Appendix D2 in Aemisegger et al., 2014). If $\Delta q < 0\,\mathrm{g\,kg^{-1}}$, q decreases compared to the previous time step, which is assumed to be due to precipitation.

- For each moisture uptake, the relative contribution to the total q of the air parcel after the uptake is calculated. If moisture loss or uptake occurs, the contribution of all previous uptakes to the total q is adjusted depending on the amount of moisture loss or uptake, respectively.

- The moisture sources for a given time along the ACE track are calculated by averaging over all trajectories weighted by the q of the air parcels upon arrival

- The conditions at the moisture source, such as longitude, latitude, time before arrival, specific humidity and the isotopic composition, identified for each trajectory are weighted by the air parcel's specific humidity upon arrival in the marine boundary layer.

Several aspects need to be considered, when using the WaterSip moisture source diagnostic in our setup:

- Due to the low q at high latitude, WaterSip is less reliable in these regions (Sodemann, 2020). The focus of this study is on the marine boundary layer, therefore, even though we are analysing moisture transport at high latitude, we do not encounter very low q as expected over, e.g., the Antarctic continent.

- No threshold for a minimal change in q between two time steps along the trajectories is chosen. This means, that also a very small Δq is interpreted as either moisture uptake or loss by the air parcel, even though a small Δq might be due to numeric noise. We conducted a sensitivity analysis, which showed that choosing a threshold above zero for Δq does not change the results for the $COSMO_{iso}$ trajectories with a temporal resolution of 1 h.

S2 1979-2018 climatology of temperature advection for the months Dec-March

In Fig. S1, the climatological advection frequency in the region south of 30° S for the period from December to March 1979 - 2018 is shown for cold temperature advection, warm temperature advection and zonal flow. The three advection regimes occur with different climatological frequencies. Zonal flow is the most frequently occurring advection regime (56 %). Cold and warm temperature advection account for 32% and 12 %, respectively. The patterns of the climatological occurrence frequency for cold and warm temperature advection are very similar to the occurrence frequencies during the ACE summer from December 2016 to March 2017 (see Fig. 5 in the manuscript). The occurrence frequencies for the zonal flow are described in more detail in the following.

The zonal flow category represents situations when air is advected zonally and ocean surface and air temperature differ by less than $\pm 1^{\circ}$C. The highest occurrence frequency of zonal advection occurs south of 60°S (Fig. S1e), where synoptic-scale fronts are rare (Simmonds et al., 2011). Furthermore, zonal flow is frequent at the equatorward edge of the highest cyclone frequency, where air is transported zonally. In the South Pacific, this band of high occurrence frequency between 60 °S and 40 °S spans particularly far north due to the northward shift of the storm track in the Pacific compared to other ocean basins (Wernli and Schwierz, 2006). The composite mean ocean evaporation is low during zonal advection and has a mean value of $0.05 \pm 0.02\,\mathrm{mm\,h^{-1}}$, i.e., between the mean values of ocean evaporation during cold and warm temperature advection (Fig. S1f). The mean value of surface precipitation during zonal flow is $0.10 \pm 0.03\,\mathrm{mm\,h^{-1}}$ and, therefore, the net moisture flux is slightly negative during zonal flow.

References

Aemisegger, F., Pfahl, S., Sodemann, H., Lehner, I., Seneviratne, S. I., and Wernli, H.: Deuterium excess as a proxy for continental moisture recycling and plant transpiration, Atmos. Chem. Phys., 14, 4029–4054, https://doi.org/10.5194/acp-14-4029-2014, 2014.

Pfahl, S. and Wernli, H.: Air parcel trajectory analysis of stable isotopes in water vapor in the eastern Mediterranean, J. Geophys. Res., 113, D20 104, https://doi.org/10.1029/2008JD009839, 2008.

Simmonds, I., Keay, K., and Tristram Bye, J. A.: Identification and climatology of southern hemisphere mobile fronts in a modern reanalysis, J. Clim., 25, 1945–1962, https://doi.org/10.1175/JCLI-D-11-00100.1, 2011.

Sodemann, H.: Beyond turnover time: Constraining the lifetime distribution of water vapor from simple and complex approaches, J. Atmos. Sci., 77, 413–433, https://doi.org/10.1175/JAS-D-18-0336.1, 2020.

Sodemann, H., Schwierz, C., and Wernli, H.: Interannual variability of Greenland winter precipitation sources: Lagrangian moisture diagnostic and North Atlantic Oscillation influence, J. Geophys. Res., 113, D03 107, https://doi.org/10.1029/2007JD008503, 2008.

Wernli, H. and Schwierz, C.: Surface cyclones in the ERA-40 dataset (1958–2001). Part I: Novel identification method and global climatology, J. Atmos. Sci., 63, 2486–2507, https://doi.org/10.1175/JAS3766.1, 2006.

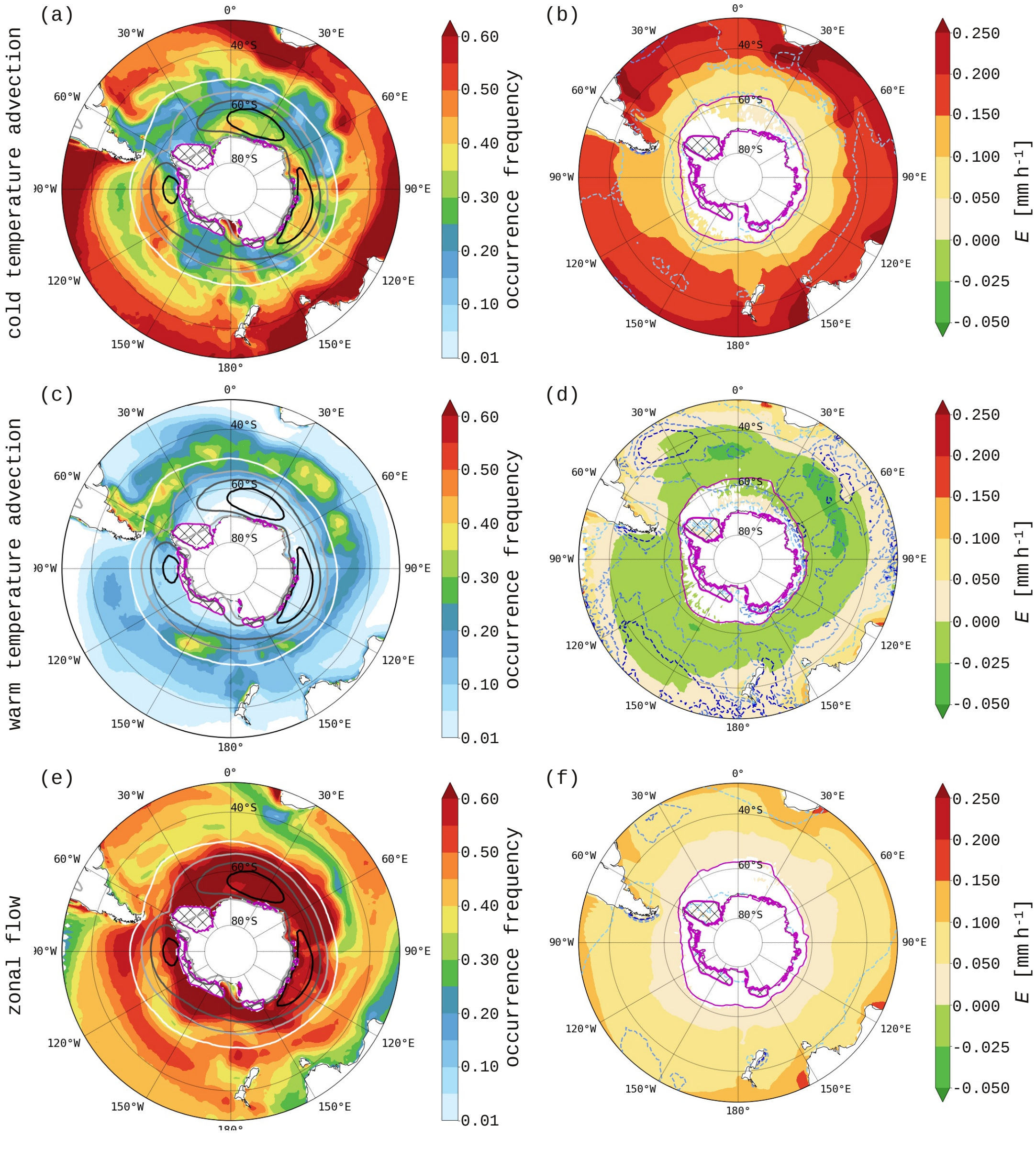

Figure S1: Climatological occurrence frequencies of cold and warm temperature advection and zonal flow **(a,c,e)** and the associated ocean evaporation **(b,d,f)** for December to March 1979-2018 using ERA-Interim. Contours in panels **a**, **c** and **e** show the cyclone frequencies of 10, 20, 30 and 40% (from white to black, respectively). Blue dashed lines in panels **b**, **d** and **f** show mean surface precipitation in the respective flow category at levels of 0.06, 0.18, 0.24, and 0.3 $\mathrm{mm\,h^{-1}}$ (from light to dark blue, respectively). Land areas and areas covered by at least 50% sea ice are blanked. Additionally, the blanked sea ice areas are hatched and bounded by pink contours. In panels **b**, **d** and **f**, the thin pink line denotes the regions, which are at least 1% covered by sea ice.